

# 2 Transverse Single-Spin Asymmetries for $\pi^0$ and 3 Electromagnetic Jets at Forward Rapidities in $p^\uparrow+p$ 4 Collisions at $\sqrt{s} = 200$ GeV and 500 GeV at STAR

5 Latiful KABIR<sup>1</sup> (for the STAR Collaboration)

6 <sup>1</sup>University of California at Riverside, Riverside, CA 92521, USA

7 E-mail: latiful.kabir@ucr.edu

8 (Received February 14, 2022)

9 There have been numerous attempts, both experimentally and theoretically, to understand the ori-  
10 gin of the unexpectedly large transverse single-spin asymmetries ( $A_N$ ) for inclusive hadron produc-  
11 tion at forward rapidity in  $p^\uparrow+p$  collisions that persist from low to high center-of-mass energies.  
12 Two potential sources are the twist-3 contributions in the collinear factorization framework and the  
13 transverse-momentum-dependent contributions from either the initial-state quark and gluon Siv-  
14 ers functions and/or the final-state Collins fragmentation function. To investigate the underlying physics  
15 leading to this large  $A_N$ , we study  $\pi^0 A_N$  with different topologies – isolated and non-isolated, and  $A_N$   
16 for electromagnetic jets (EM-jets) of different substructures using the Forward Meson Spectrometer  
17 (FMS) at STAR. Jet  $A_N$  is sensitive to the initial-state effect and can provide access to Siv-  
18 ers functions. To investigate final-state effects, we measure the Collins asymmetry of  $\pi^0$  inside EM-jets. We  
19 present the most recent results for these asymmetries from  $p^\uparrow+p$  collisions at 200 GeV and 500 GeV.  
20 We also present new preliminary results of  $A_N$  for EM-jets in the FMS and Endcap Electromagnetic  
21 Calorimeter (EEMC) using  $p^\uparrow+p$  collisions at 200 GeV, where we explore the dependences of  $A_N$   
22 on photon multiplicity inside the jet, jet transverse momentum, and jet energy. These results provide  
23 rich information towards understanding the physics mechanism of large  $A_N$  in hadronic collisions.

7 **KEYWORDS:** TSSA, TMD, EM-jet

## 8 1. Introduction

9 Transverse Single-Spin Asymmetry (TSSA or  $A_N$ ) in hadron-hadron collisions plays an important  
10 role in understanding the QCD structure of the nucleon.  $A_N$  is defined as the left-right asymmetry of par-  
11 ticle production relative to the plane defined by the momentum and spin directions of a polarized hadron.  
12 pQCD predicts this asymmetry to be small [1], however, this turned out to be unexpectedly large for the  
13 forward hadron production in  $p^\uparrow+p$  collisions which has been verified by fixed target and collider exper-  
14 iments, including experiments at Fermilab and RHIC [2] - [5]. The origin of this large asymmetry is an  
15 unsolved puzzle for the last 40 years. There have been various attempts, both experimentally and theoret-  
16 ically, to understand the origin of large  $A_N$  for inclusive hadron production at forward rapidity in  $p^\uparrow+p$   
17 collisions. On the theoretical side, two potential sources are the twist-3 contributions in the collinear  
18 factorization framework and the transverse-momentum-dependent (TMD) contributions from either the  
19 initial-state quark and gluon Siv-  
20 ers functions and/or the final-state Collins fragmentation function. Also,  
21 there are some indications from data that diffractive processes might have a non-trivial contribution to  
22 the large  $A_N$  [6]. In the TMD framework, for the Siv-  
23 ers mechanism, the asymmetry comes from the  
correlation between the proton spin and the parton transverse momentum. In analogy, the Collins effect  
comes from the correlation between the quark spin and the hadron transverse momentum in jets. For the

twist-3 contribution, the source is the quark-gluon or gluon-gluon correlations and fragmentation functions. On the experimental side, the focus has been on measuring the signatures for the Sivers effects or Collins effects to disentangle the initial-state or final-state effects, and searching for possible other sources.

In 2011 and 2015, STAR collected data for transversely polarized  $p^\uparrow + p$  collisions at  $\sqrt{s} = 200$  and 500 GeV, which are ideal to further characterize  $A_N$  and explore its potential sources. The STAR Forward Meson Spectrometer (FMS) and Endcap Electromagnetic Calorimeter (EEMC), having full azimuthal coverages and pseudo-rapidity ( $\eta$ ) coverages of 2.6 - 4.2 and 1.1 - 2.0 respectively, can be used to detect photons, neutral pions, and eta mesons. We present  $\pi^0 A_N$  with different event topologies and  $A_N$  for EM-jets using the FMS. In addition, we present the new preliminary results for  $A_N$  of EM-jets in the FMS and EEMC using  $p^\uparrow + p$  collisions at  $\sqrt{s} = 200$  GeV. For the latter analysis, we present the dependences of  $A_N$  on photon multiplicity inside the jet, jet transverse momentum ( $p_T$ ), and jet energy. A jet in the context of our analysis is always an EM-jet reconstructed from photons only.

## 2. Analysis Method

The datasets used are for transversely polarized  $p^\uparrow + p$  collisions at  $\sqrt{s} = 500$  and 200 GeV with average beam polarizations of 52% and 57% and integrated luminosities of 25  $\text{pb}^{-1}$  and 52  $\text{pb}^{-1}$ , respectively. Events are triggered based on the energies deposited in a cluster of towers or a jet patch sensitive to  $\pi^0$ s and jets in the calorimeters. A jet patch is formed by grouping calorimeter regions together. For Monte Carlo, we use PYTHIA 6.428 event generator with Perugia 2012 Tune. Events generated by PYTHIA are propagated through GEANT-based STAR detector simulation to simulate the detector response.

In the FMS, photon candidates are reconstructed by finding clusters of continuous energy depositions. Two photons are then combined to reconstruct  $\pi^0$  candidates. Selected  $\pi^0$ s are required to have  $p_T > 2.0$  GeV/c,  $M_{\gamma\gamma} < 0.3$  GeV/c<sup>2</sup> and  $Z_{\gamma\gamma} = \frac{|E_1 - E_2|}{E_1 + E_2} < 0.7$ , where  $E_1$  and  $E_2$  are the energies of the photon pair. Jets are reconstructed in the FMS or EEMC using the anti- $k_T$  algorithm from the FastJet package [11] with a radius of 0.7. Reconstructed photons are used as inputs to FastJet for reconstructing EM-jets in the FMS. For EM-jets in the EEMC, towers are used as inputs. Individual photons are required to have  $E_\gamma > 1.0$  GeV (FMS) or  $E_T > 0.2$  GeV (EEMC). The jets are required to have  $p_T$  greater than 2.0 GeV/c.

The measured or raw asymmetry ( $\epsilon$ ) is related to  $A_N$  by the cosine modulation ( $\cos \phi$ ) with a correction for the polarization ( $P$ ) as shown in Eq. 1, where  $\phi$  is the azimuthal angle of the  $\pi^0$  or EM-jet in the lab frame. We calculate the raw asymmetry using the cross-ratio formula shown in Eq. 2, where  $N_{\phi(\phi+\pi)}^{\uparrow(\downarrow)}$  is the number of  $\pi^0$ s or EM-jets detected at  $\phi$  ( $\phi + \pi$ ) for spin up (down) state. It cancels systematics coming from the relative luminosity and the detector efficiency. To extract the  $A_N$  from raw asymmetry, we fit it with a cosine function. The left plot in Fig. 1 shows one example fit for a particular jet energy,  $p_T$ , and photon multiplicity bin. The  $\chi^2$  distribution from all fits shows the overall quality of the fit for the EM-jet  $A_N$  extraction.

$$\epsilon = PA_N \cos(\phi) \quad (1)$$

$$\epsilon \approx \frac{\sqrt{N_\phi^\uparrow N_{\phi+\pi}^\downarrow} - \sqrt{N_{\phi+\pi}^\uparrow N_\phi^\downarrow}}{\sqrt{N_\phi^\uparrow N_{\phi+\pi}^\downarrow} + \sqrt{N_{\phi+\pi}^\uparrow N_\phi^\downarrow}} \quad (2)$$

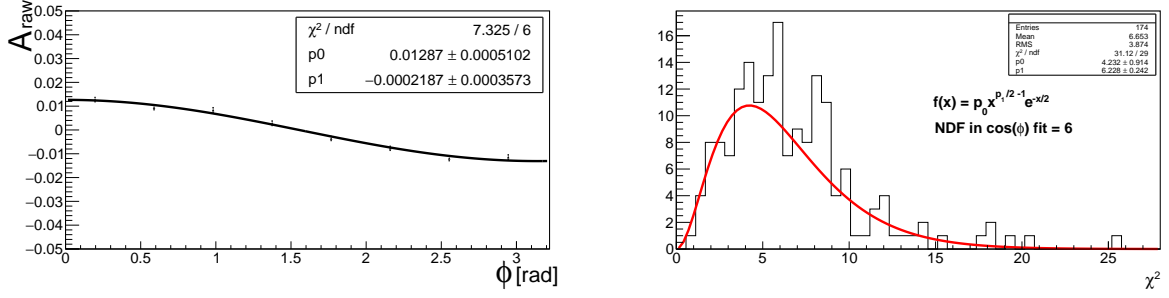


**Fig. 1.** (Left) Example of fitting the raw asymmetry with  $p_0 \cos(\phi) + p_1$  for EM-jets with 2 photons, 20 GeV  $< E_{jet}^{EM} < 40$  GeV and  $2.5 \text{ GeV}/c < p_T < 3.0 \text{ GeV}/c$ . (Right)  $\chi^2$  distribution from all fits showing overall quality of the fit for EM-jet  $A_N$  extraction using 200 GeV FMS data.

### 3. Results

The results for  $A_N$  of  $\pi^0$  at 200 GeV and 500 GeV using the FMS are presented in Fig. 2 (left). We find that  $A_N$  for isolated  $\pi^0$  is significantly larger than  $A_N$  of non-isolated  $\pi^0$ . An isolated  $\pi^0$  is a  $\pi^0$  without any energy deposited around it. The theoretical calculations, shown in solid curves, are based on the latest global fit [8]. Figure 2 (right) shows EM-jet  $A_N$  results at 200 GeV and 500 GeV using

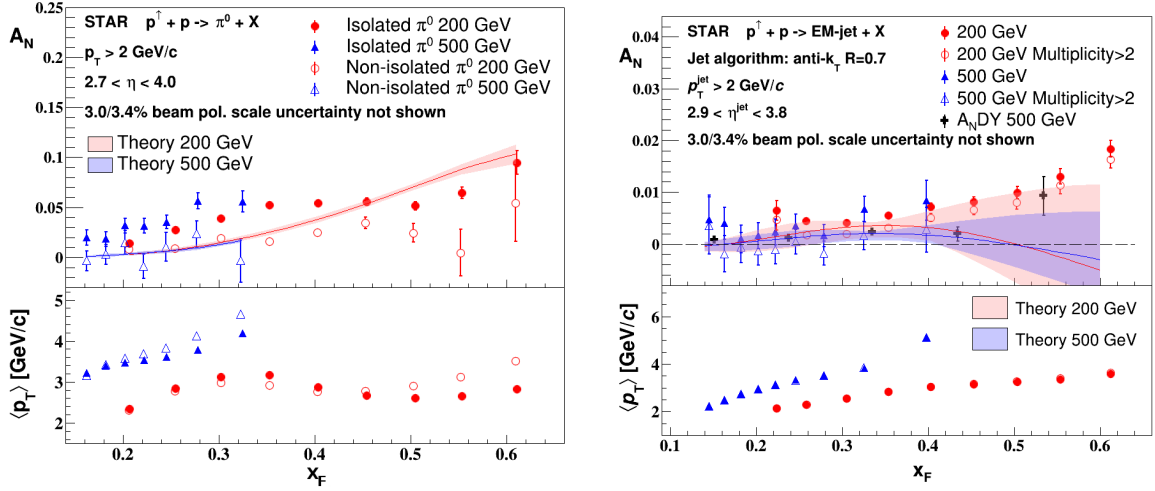


**Fig. 2.** (Left)  $A_N$  as a function of longitudinal momentum fraction, Feynman- $x$  ( $x_F$ ), for the isolated and non-isolated  $\pi^0$  in transversely polarized  $p^\dagger + p$  collisions at 200 and 500 GeV [6]. The average  $p_T$  of the  $\pi^0$  for each  $x_F$  bin is plotted in the lower panel. (Right) EM-jet  $A_N$  as a function of  $x_F$  in polarized  $p^\dagger + p$  collisions at 200 and 500 GeV [6]. Results with at least three photons inside an EM-jet are shown as open circles. Previous results by the  $A_NDY$  Collaboration are also plotted in black solid points. The theory curves shown are for TSSA of the full jets at  $\langle y \rangle = 3.25$  for 200 GeV and  $\langle y \rangle = 3.57$  for 500 GeV. The average  $p_T$  of the EM-jet for each  $x_F$  bin is shown in the lower panel.

the FMS. We find that EM-jet  $A_N$  is small compared to  $\pi^0 A_N$ . EM-jets with more than 2 photons have smaller asymmetries than EM-jets consisting of 1 or 2 photons. The impact of this forward EM-jet  $A_N$  result on up and down quark Sivers functions has been recently presented in [7]. Figure 3 shows the Collins asymmetry for  $\pi^0$  in a jet at 200 GeV and 500 GeV. In the figure,  $z_{em}$  is given by  $z_{em} = \frac{E_\pi}{E_{jet}}$ . The Collins asymmetries are found to be very small at both energies. We also find weak  $j_T$  dependence,

70 where  $j_T$  is the  $\pi^0$  transverse momentum relative to the jet axis. Details on the results in Figs. 2 and 3  
 71 and related discussions can be found in Ref. [6].

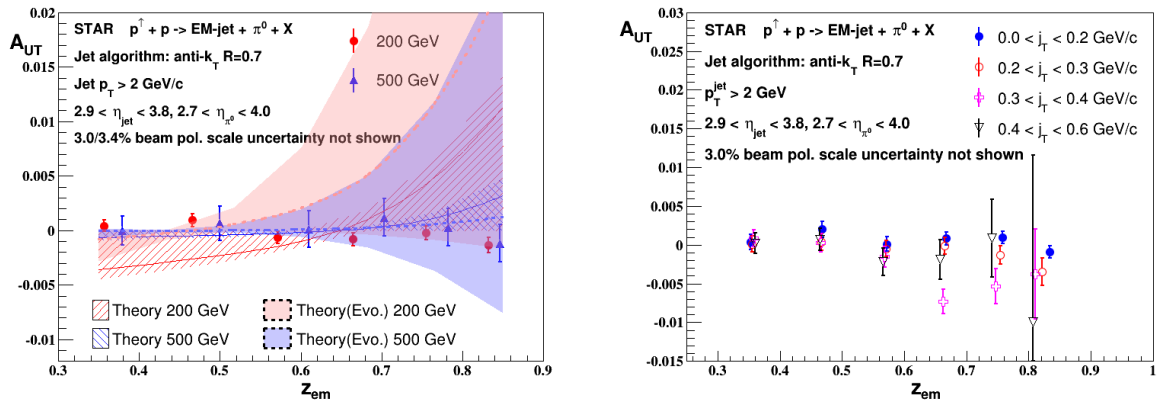


**Fig. 3.** (Left) The Collins asymmetry for  $\pi^0$ s in an EM-jet for transversely polarized  $p^\uparrow+p$  collisions at 200 GeV and 500 GeV [6]. The theory curves shown are for the Collins asymmetry of  $\pi^0$ s in a full jet with or without the TMD evolution [9]. (Right) The  $j_T$  dependence of the Collins asymmetry in transversely polarized  $p^\uparrow+p$  collisions at 200 GeV.

72 To investigate the substructure dependence of  $A_N$ , we carry out a detailed analysis of photon-  
 73 multiplicity dependence of EM-jet  $A_N$  at forward rapidity using the FMS in  $p^\uparrow+p$  collisions at  $\sqrt{s} = 200$   
 74 GeV. Figure 4 shows EM-jet  $A_N$  at the forward rapidity (FMS) for the cases:  $n_\gamma \leq 2$  (red),  $n_\gamma = 3$   
 75 (black) and  $n_\gamma \geq 4$  (open circle). We find that  $A_N$  increases with increasing  $x_F$ . EM-jet  $A_N$  is the  
 76 strongest for EM-jets consisting of 1 or 2 photons. EM-jets with 3 photons have a non-zero  $A_N$  but lower  
 77 than that of 1-photon or 2-photon EM-jets. EM-jets with higher photon multiplicities have significantly  
 78 smaller asymmetries.

79 Next, we perform a multi-dimensional analysis to demonstrate the dependences of  $A_N$  on  
 80 photon multiplicity inside the jet, jet transverse momentum, and jet energy. The results obtained  
 81 using  $p^\uparrow+p$  collisions at  $\sqrt{s} = 200$  GeV are presented in Fig. 5. The left plot shows the results at  
 82 forward rapidity using the FMS. For  $x_F > 0$ , we observe that EM-jet  $A_N$  decreases with increas-  
 83 ing photon multiplicity (“jettiness”), i.e.  $A_N$  is the  
 84 strongest for EM-jets consisting of 1 or 2 photons and significantly smaller for EM-jets with 4  
 85 or 5 photons.  $A_N$  at  $x_F < 0$  is found to be consistent with zero regardless of the photon multi-  
 86 plicity. These results are consistent with our previous measurement at 500 GeV [10]. The right  
 87 plot shows the results at the intermediate rapidity measured using the EEMC.  $A_N$  is zero at low  $p_T$   
 88 and positive at higher  $p_T$  for  $x_F > 0$ .  $A_N$  is sig-  
 89 nificantly smaller for EM-jets at the intermediate rapidity, probing a much lower  $x_F$  range, compared  
 90 to forward rapidity. The trend of EM-jet  $A_N$  decreasing with increasing photon multiplicity (“jettiness”)  
 91 seems to hold.  $A_N$  at  $x_F < 0$  is consistent with zero. Here, the systematic uncertainties (rectangular  
 92 boxes  
 93  
 94  
 95  
 96  
 97  
 98  
 99

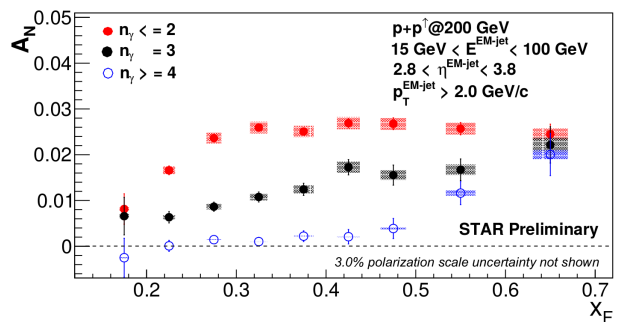


**Fig. 4.** EM-jet  $A_N$  at the forward rapidity (FMS) for the cases:  $n_\gamma \leq 2$  (red),  $n_\gamma = 3$  (black) and  $n_\gamma \geq 4$  (open circle). The systematic uncertainties (rectangular) come from possible misidentification of the event category.

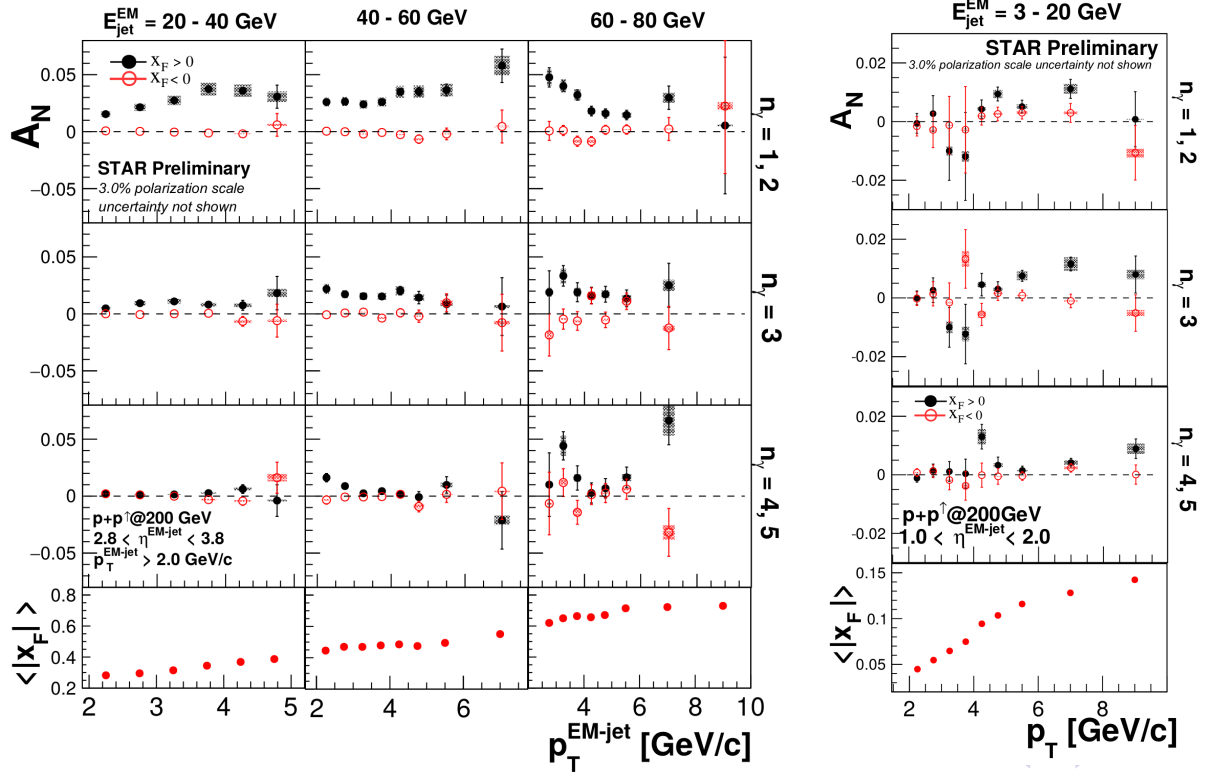


**Fig. 5.** (Left)  $A_N$  for EM-jets at the forward rapidity (FMS) sorted by photon multiplicity inside the jet and different  $p_T$  and energy bins. (Right) EM-jet  $A_N$  at the intermediate rapidity (EEMC) as a function of  $p_T$  sorted by EM-jet photon multiplicity. The lowermost panels show average  $x_F$  for each  $p_T$  bin.

around data points) arise from possible misidentification of the event category.

## 4. Conclusion

We present  $\pi^0 A_N$  with different topologies and  $A_N$  for EM-jets using the FMS at STAR in  $p^\uparrow + p$  collisions at  $\sqrt{s} = 200$  GeV and 500 GeV.  $A_N$  for isolated  $\pi^0$  is significantly larger than  $A_N$  of non-isolated  $\pi^0$ . The Collins asymmetry is found to be small. We also study  $A_N$  for EM-jets of different substructures using the FMS and EEMC at STAR in 200 GeV  $p^\uparrow + p$  collisions. EM-jet  $A_N$  decreases with increasing photon multiplicity (“jettiness”). These results provide rich information towards understanding the physics mechanism of large  $A_N$  in hadronic collisions.

## References

- [1] Kane, Pumplin and Repko, Phys. Rev. Lett. **41** 1689 (1978).
- [2] D.L. Adams *et al.*, Phys. Lett. B **261**, 201(1991)
- [3] B. I. Abelev *et al.*, Phys. Rev. Lett. **101**, 222001(2008)
- [4] A. Adare *et al.*, Phys. Rev. D **90**, 012006 (2014)
- [5] E.C. Aschenauer *et al.*, arXiv:1602.03922
- [6] J. Adam *et al.*, Phys. Rev. D **103**, 092009 (2021)
- [7] M. Boglione *et al.*, Phys. Lett. B **815**, 136135 (2021)
- [8] J. Cammarota *et al.*, Phys. Rev. D **102**, 054002 (2020)
- [9] Z.-B. Kang, *et al.*, Phys. Lett. B **774**, 635 (2017)
- [10] M.M. Mondal (STAR Collaboration) PoS (DIS2014) 216
- [11] M. Cacciari and G.P. Salam, Phys. Lett. B **641** (2006) 57